Vol. 37, No. 2 (2015) 176-185

Tribology in Industry

www.tribology.fink.rs

RESEARCH

A Comparative Experimental Study on Identification of Defect Severity in Rolling Element Bearings using Acoustic Emission and Vibration Analysis

V.V. Rao[a], Ch. Ratnam[b]

[a]*Engineering Shops Department, Visakhapatnam Steel Plant, Visakhapatnam, AP, India*,

[b]*Department of Mechanical Engineering, Andhra University, Visakhapatnam, AP, India.*

Keywords:

Roller Bearings
Characteristic defect frequency
Vibration analysis
Acoustic emission

Corresponding author:

V. Vital Rao
Engineering Shops Department,
Visakhapatnam Steel Plant,
Visakhapatnam, AP, India.
E-mail: vvrao_vana@yahoo.co.in

A B S T R A C T

This paper describes the comparison between Vibration Analysis (VA) and Acoustic Emission (AE) method to predict the defect severity in rolling element bearings with respect to the gradual increase of defect size. In bearing fault diagnosis vibration based methods are very popular, but the signals acquired by its transducers from the bearings are distorted by other faults and mechanical noise from the equipment. Vibration based methods are effective when the defect in the bearings has already become severe. AE is a non destructive testing (NDT) technique used in structural health monitoring and its application for bearing defect diagnosis is gaining momentum as an alternate diagnostic tool because of its inherent high signal-to-noise-ratio (SNR). A bearing test rig was designed and set up to study the various defects in rolling element bearings in real environment. In earlier cases, though the researchers studied on different types of seeded defects with random sizes, they could not ascertain the correlation between their defect sizes and the vibration amplitude. The experimental investigation reported in this paper is centered on seeded defect of same type with gradual increase of its size on outer race of radially loaded cylindrical roller bearings and running the defective bearing at different speeds and loads. Data acquired through AE & vibration probes simultaneously for better diagnosis. Comparisons between AE and VA over a range of speed and load conditions at gradual increase of defect size are presented and from them it is concluded that AE method is superior to identify the severity of defect.

1. INTRODUCTION

Since failures in engineering structures can lead to severe economic loss, its health monitoring is very essential particularly in aerospace, civil, marine and other structures to avoid premature failures. Precise incipient structural damage identification and its location is of great interest to many researchers [1-5]. In rotating machinery early fault detection of the rolling elements, i.e.

bearing and gear faults has been gaining importance in recent years because of its detrimental influence on the reliability of equipment. Different techniques have been developed for monitoring and diagnosis of rolling element bearings [6]. Most of the fault detection methods are based on vibration signal analysis and it is the commonly used technique employed in rotor-bearing systems. Todorovic Petar et al. [7] studied vibration analysis of cracked rotor system to find out the fatigue cracks. Detection of the fault and its severity are two important steps or features of a condition monitoring system. Lifetime of a machine component is determined by the severity of the fault. It is crucial, especially in critical systems, where continual operation is generally indispensable. The bearing defects can be either distributed or local type or combination of both. The distributed defects can be due to surface roughness, waviness, misaligned races, and off-size rolling elements. Localized defects are developed in the raceways, rollers and cage of a bearing. The periodic impacts occur at ball-passing frequency (characteristic defect frequencies), which can be estimated from the bearing geometry and the rotational speed [8]. The vibration signal is not sensitive to the incipient defects in the bearings; sometimes the defect frequencies are not observable with the help of the Fast Fourier Transform (FFT) spectrum, because the impulses generated by the defects are masked or distorted by the noise generated by other parts of the equipment. To overcome this problem, advanced signal processing techniques are implemented by many researchers to detect bearing local faults [9].

Acoustic emissions are actually defined as transient elastic waves generated from a rapid release of strain energy caused by a deformation or damage within or on the surface of a material [10]. AE was originally developed for non-destructive testing of static structures; however its applications have now been extended to condition monitoring of rotating machines. During the last few years, a significant progress in the capabilities of acoustic instrumentation together with the signal processing techniques has made it possible to extract useful diagnostic information from acoustic signals. AE signals are used in tribological studies to study the friction and wear of coated machine components [11]. AE analysis, gives valuable information about origin of damages at the contact between a PVD coating and a substrate in the body [12].

The interaction of surface asperities and impingement of the bearing elements over the defect on the race pathway generates acoustic emissions which are basically transient elastic waves. There have been numerous investigations reported on applying AE to bearing defect diagnosis. Some investigators [13-15] have shown that certain AE parameters identified bearing defects before they appeared in the vibration acceleration range. In addition to this, successful applications of AE to bearing diagnosis on extremely slow rotational speeds have been reported [16,17]. The modulation of AE signatures at bearing defect frequencies has also been observed by other researchers [18-21]. AE components such as time and frequency in highly transient signals are very much dependent on each other. This prompted many researchers to work on automatic defect identification using wavelet algorithm [22,23]. Abdullah et al. [24] reported relationship between AE R.M.S. amplitude and kurtosis for a range of defect conditions and relationship between the defect size and AE burst duration. In this paper the bearing kinematics, bearing testing facility and the details of experimental investigation of both acoustic emission and vibration analysis on test bearings simultaneously for various defect sizes in outer race are reported and the results obtained are thoroughly discussed.

2. BEARING KINEMATICS

When a faulty bearing is in use, the rolling element comes across the defect, it hits the edge of the defect and produces impulse in the races. The periodic impulses produce certain frequencies (Characteristic defect frequencies). These frequencies depend on bearing kinematics, its geometry and speed.

The Fig. 1 shows schematic of a typical angular contact rolling element bearing. As a general case; it will be initially assumed that both inner and outer races rotate in a bearing which has a common contact angle and no skidding of rolling elements between the races.

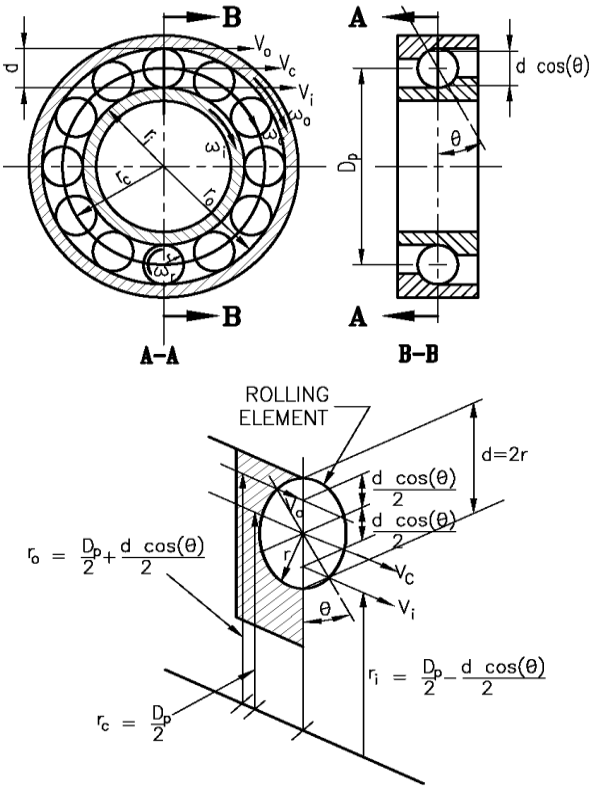

Fig. 1. Schematic diagram of bearing geometry.

v, *ω*, *f*, *r* - *refers* to linear speed, angular speed, frequency and radius.
Subscripts: *i, o, c, r* – refers to inner race, outer race, cage and rolling element.
D_p - Pitch circle diameter; d -Diameter of the rolling element; θ -Contact angle; N - Number of rolling elements.

The cage linear speed can be given by

$$v_c = \frac{v_i + v_o}{2} = \frac{\omega_i r_i + \omega_o r_o}{2} \quad (1)$$

$$r_c = \frac{D_p}{2} \quad (2)$$

$$r_i = \frac{D_p}{2} - \frac{d\cos\theta}{2} \quad (3)$$

$$r_o = \frac{D_p}{2} + \frac{d\cos\theta}{2} \quad (4)$$

From the above equations, the cage angular speed:

$$\omega_c = \frac{v_c}{r_c} \quad (5)$$

$$\omega_c = \frac{1}{2}\left[\omega_i\left(1 - \frac{d\cos\theta}{D_p}\right) + \omega_o\left(1 + \frac{d\cos\theta}{D_p}\right)\right] \quad (6)$$

$$\omega_c = 2\pi f_c$$

Fundamental Train Frequency (FTF) can be derived from the above equations and expressed in Hertz (Hz) as:

$$FTF = f_c = \frac{1}{2}\left[f_i\left(1 - \frac{d\cos\theta}{D_p}\right) + f_o\left(1 + \frac{d\cos\theta}{D_p}\right)\right] \quad (7)$$

The peak frequency appears in the frequency spectrum when the bearing rotating with an unbalanced cage and rotating elements. The frequency of rotation of the rolling elements with respect to the outer race i.e., Ball Pass Frequency of the Outer race (BPFO) can be derived by multiplying the number of rolling elements(N) with the relative angular speed between cage and outer race.

$$BPFO = N(\omega_c - \omega_o) \quad (8)$$

$$= N\left[\frac{1}{2}\left\{f_i\left(1 - \frac{d\cos\theta}{D_p}\right) + f_o\left(1 + \frac{d\cos\theta}{D_p}\right)\right\} - f_o\right] \quad (9)$$

$$= \frac{N}{2}(f_i - f_o)\left(1 - \frac{d\cos\theta}{D_p}\right) \quad (10)$$

In the similar way Ball Pass Frequency of the Inner race (BPFI) can be evaluated multiplying the number of rolling elements with the relative angular speed between cage and inner race:

$$BPFI = N(\omega_i - \omega_c) \quad (11)$$

$$= \frac{N}{2}(f_i - f_o)\left(1 + \frac{d\cos\theta}{D_p}\right) \quad (12)$$

The frequency of rotation of the rolling elements about their own axes Ball Spin Frequency (BSF), can also be derived. The frequency of rotation, assuming no slip, is given by the frequency of rotation of the cage with respect to the inner race multiplied with the diameter ratio of the inner race to the ball diameter.

The ball or roller angular speed rotating on its own centre is given as follows:

$$\omega_r = \frac{v_r}{r_r} \quad (13)$$

The ball or roller tangential speed at the contact point with the inner race is:

$$v_r = (\omega_i - \omega_c) r_i \ , \ \omega_r = \frac{(\omega_i - \omega_c)}{r_r} r_i \quad (14)$$

$$BSF = f_r = \frac{D_p}{2d}(f_i - f_o)\left[1 - \left(\frac{d\cos\theta}{D_p}\right)^2\right] \quad (15)$$

These calculated frequencies obtained may slightly vary from the actual values due to slipping or skidding of rolling elements [25]. Some researchers [26] mentioned that it is difficult to obtain a significant peak at these defect frequencies in the direct vibration spectrums obtained from a defective bearing. This is due to the fact that noise or vibration from other sources masks the vibration signal from the bearing unless the defect is sufficiently large.

3. EXPERIMENTAL SETUP

A bearing test rig is designed and setup to fulfill the requirements of current investigation and future research in this area. The schematic of the test rig is shown in Fig. 2. The testing involves mounting and running the defective bearing along with acquisition of AE and vibration signal data under various speed and load conditions.

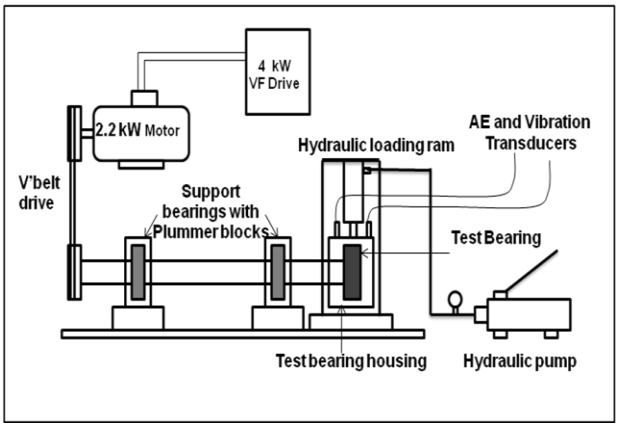

Fig. 2. Schematic of experimental test rig.

Fig. 3. Bearing Test Rig.

The test rig (Fig. 3) consists of six major parts i.e. shaft, support bearings with plumber blocks, bearing block with test bearing, 2.2 kW-3 phase induction motor, 4 kW variable frequency drive to control speed, and a vertical hydraulic ram for applying load radially. The operational speed range is up to 2800 rpm with a maximum load capability of 16 kN via a hydraulic ram. On one end of the shaft a V-pulley and on the other end a test bearing with housing is assembled. The shaft is supported by two bearings with plumber blocks. Deep groove ball bearings (SKF 6212 RS2) concealed on both sides are used as support bearings. The motor drives the shaft with a V-belt. The motor is mounted on a separate base frame to avoid transfer of vibration to test rig. The test bearing block is square split housing and is made of EN 24 steel material. On top of split housing, AE probe, vibration accelerometer and hydraulic ram are placed while conducting the test run.

4. EXPERIMENT METHODOLOGY

In this investigation N 312 type cylindrical roller bearing with normal clearance is used (Fig. 4). The geometric details of the test bearing are, Inner diameter- 60 mm, Outer diameter- 130 mm, Width- 33 mm, Number of rollers- 12, Rolling element diameter- 18 mm, Pitch circle diameter (D_p)- 96 mm, Contact angle (θ)- 0^0. The reason for selection of this bearing is that it allows easy assembly and dismantling of outer race and defect creation for investigation.

Fig. 4. N312 cylindrical roller bearing.

Fig. 5. Outer race seeded defect (0.5 mm width) & Test bearing housing.

Total five N312 bearings with defect width of various sizes (0.3, 0.5, 0.7, 0.9, and 1.1 mm) are

used in this study. Fig. 5 shows 0.5 mm width defect on outer race of bearing. A defect of depth 0.3 mm was maintained in all test bearings.

For acoustic emission data acquisition, MHC-memo pro (Holroyd make) AE instrument with magnetic mount sensor of model 1030 Mag is used. 2048 samples (data points) are recorded per sec for each time wave. For vibration data, CSI 2120 model vibration analyzer with triaxial accelometer with integral magnet (model A0643TX) is used. 1024 data samples per sec is its sampling frequency.

A good bearing without any defect is assembled in the test bearing housing and the test rig is run for minor adjustments. After that, the defect seeded bearing is assembled in the test bearing housing and the defect is positioned at the top where the load is applied radially through hydraulic ram. All the test runs are conducted at two loads in 2 kN and 4 kN at different speeds varying from 500 to 1500 RPM in six steps. The same process is repeated for the other defect seeded bearings. In the present study AE and vibration data are recorded simultaneously in all test runs for better comparison.

5. RESULTS AND DISCUSSION

Characteristic defect frequencies of N312 bearing are calculated theoretically for all the speeds planned in test runs and are presented in Table. 1.

Table 1. Theoretical Characteristic defect frequencies at different speeds.

RPM		500	700	900	1100	1300	1500
Defect frequency in Hertz	FTF	3.39	4.74	6.09	7.45	8.80	10.06
	BSF	21.43	30.03	38.59	47.16	55.76	64.32
	BPFI	59.35	83.15	106.88	130.60	154.40	178.13
	BPFO	40.61	56.89	73.13	89.36	105.64	121.88

The AE and vibration signal data is processed through FFT with respect to AE lab software and CSI vibration analysis software. Time waves and frequency spectrums at all test runs are analyzed in detail for comparative study and presented. Some of the time waves and frequency spectrums of acoustic emission are presented in Figs. 8-12.

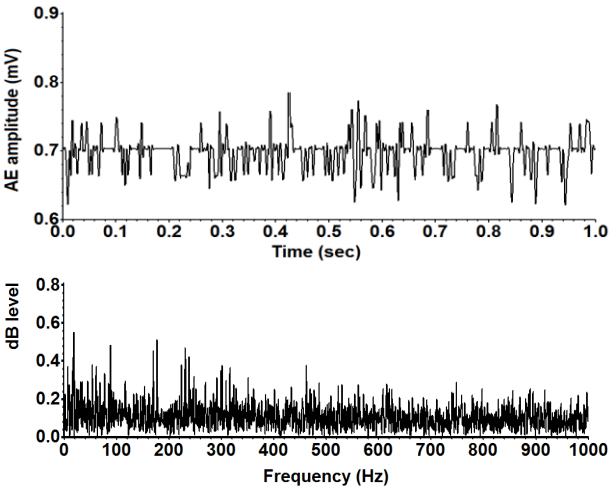

Fig. 8. AE Time wave & Frequency spectrum without defect, 4 kN load, 1500 RPM.

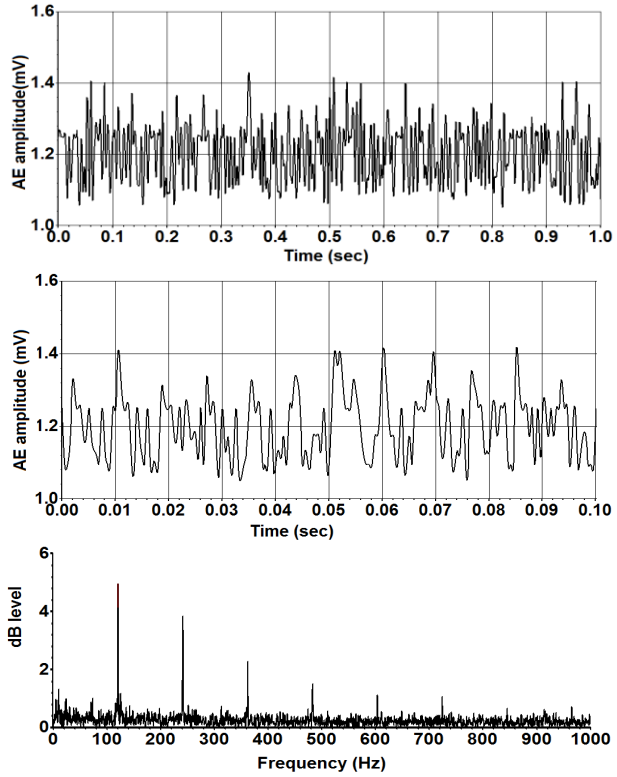

Fig. 9. AE Time wave & Frequency spectrum with 0.5 mm defect, 4 kN load, 1500 RPM.

Figure 8 shows AE time wave and envelope frequency spectrums of test run conducted with good bearing. No significant peaks are observed at any defect frequency. Figures 9-12 shows the time waves and frequency spectrums of test runs conducted with different defect sizes at same speed & load conditions. In all frequency spectra the peaks are raised only at frequency 121.88 Hz (BPFO), and its subsequent super-harmonics and no other peaks were observed. In the expanded time waves it is noticed that there

are 12 impulses recorded for every 0.1 sec which matches with its BPFO. The peak width increases with increase of defect size and gives clear idea about the defect size increment. In vibration spectrums (Figs. 13 to 16) there is no such clear peak observed at outer race defect frequency.

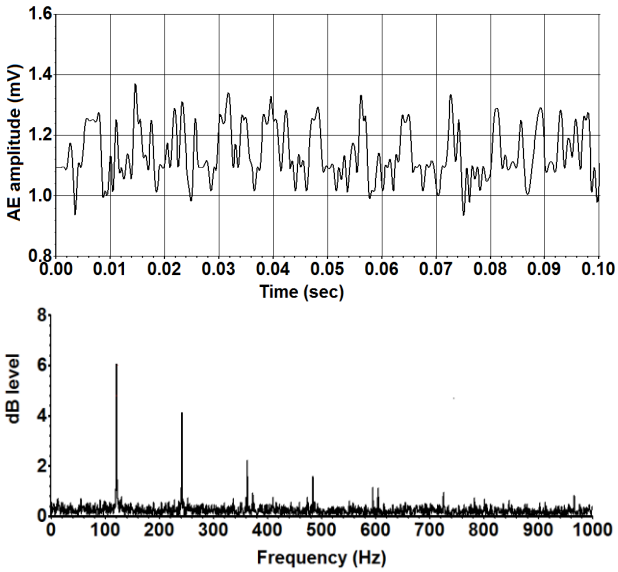

Fig. 10. AE Time wave & Frequency spectrum with 0.7 mm defect, 4 kN load, 1500 RPM.

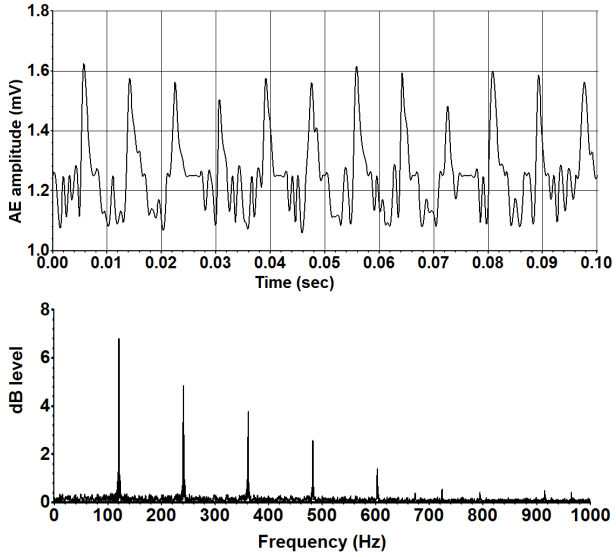

Fig. 11. AE Time wave & Frequency spectrum with 0.9 mm defect, 4 kN load, 1500 RPM.

In vibration frequency spectrum at low RPM the peak at outer race frequency not observed. At higher RPM more than 900 the defect peak is observed but other peaks dominate it and masks the defect frequency.

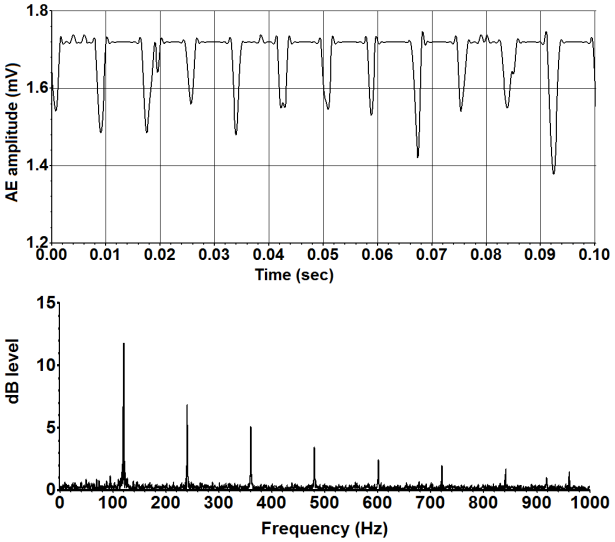

Fig. 12. AE Time wave & Frequency spectrum with 1.1 mm defect, 4 kN load, 1500 RPM.

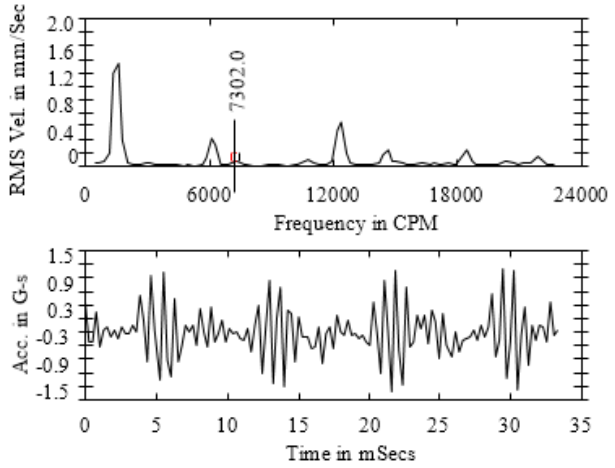

Fig. 13. Vibration Frequency spectrum & Time wave (1500 RPM, 4 kN load, 0.5 mm width defect).

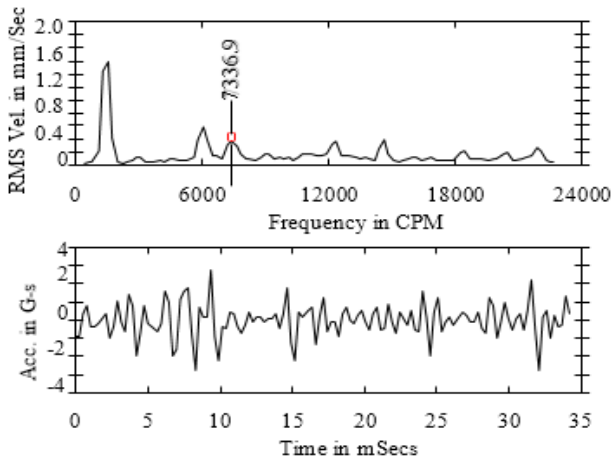

Fig. 14. Vibration Frequency spectrum & Time wave (1500 RPM, 4 kN load, 0.7 mm width defect).

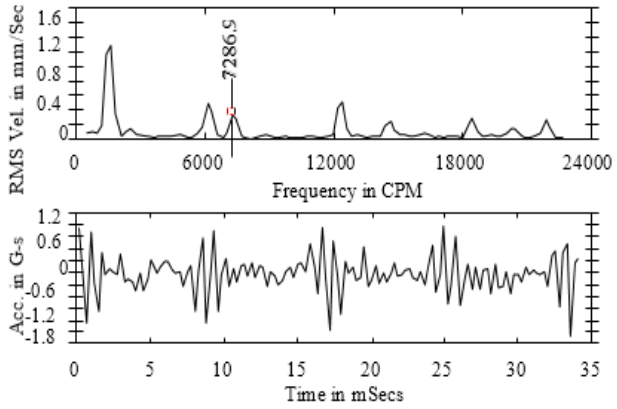

Fig. 15. Vibration Frequency spectrum & Time wave (1500 RPM, 4 kN load, 0.9 mm width defect).

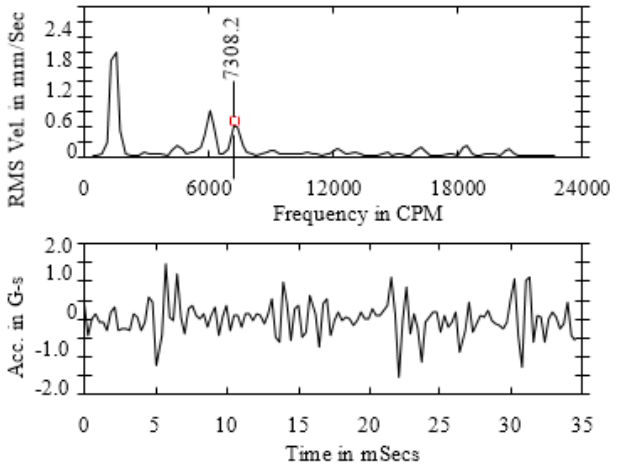

Fig. 16. Vibration Frequency spectrum & Time wave (1500 RPM, 4 kN load, 1.1 mm width defect).

In Table 2, AE amplitudes (dB level) at defect frequencies for a good bearing and a defective bearing (0.5 mm width defect at outer race) under 2 kN load are presented. In the test run with a good bearing, minimum AE amplitude values are shown at all defect frequencies but with a defective bearing these values are high at BPFO compared to other frequencies. This indicates that outer race defect shows a gradual increasing trend with increase in RPM.

Table 2. Acoustic Emission amplitude (dB level) at defect frequencies, 2 kN load.

RPM	Without defect				0.5 mm width defect at outer race			
	FTF	BSF	BPFI	BPFO	FTF	BSF	BPFI	BPFO
500	0.11	0.25	0.26	0.29	0.57	0.18	0.13	1.14
700	0.07	0.17	0.11	0.30	0.68	0.76	0.35	1.46
900	0.15	0.35	0.56	0.46	0.31	0.77	0.57	2.16
1100	0.07	0.32	0.27	0.24	0.28	0.43	0.09	2.89
1300	0.06	0.52	0.54	0.35	0.26	0.51	0.24	3.21
1500	0.17	0.58	0.28	0.15	0.56	0.55	0.04	3.52

The Table 3 shows the AE dB levels at actual BPFO taken from AE envelope spectra at defect size 0.5mm and two load conditions 2 kN and 4 kN. The theoretical and actual BPFO at different RPM are presented. Actual BPFO is less than the theoretical defect frequencies. The difference in theoretical and actual BPFO at 4 kN load is shown in Table 3. This difference was observed by many researchers in vibration analysis [22, 23]. It is due to slippage and skidding of rolling element while running in its path. It is also observed in AE analysis. The difference in BPFO increases with increase in speed but there is no significant change with increase in load.

Table 3. AE amplitude (dB level) values at actual BPFO at outer race defect bearing.

RPM	Theoretical BPFO	0.5 mm defect				Difference in BPFO
		2 kN Load		4 kN Load		
		dB value	Actual BPFO	dB value	Actual BPFO	
500	40.61	1.80	40.016.	2.04	40.504	0.106
700	56.89	1.46	56.608	3.43	56.608	0.282
900	73.13	2.16	72.224	4.32	72.224	0.906
1100	89.36	2.89	88.328	5.84	88.328	1.032
1300	105.64	3.21	104.432	4.21	104.432	1.208
1500	121.88	3.52	120.536	5.07	120.536	1.344

Table 4. Vibration RMS velocity in (mm/sec) at various defect sizes, RPM and Load.

RPM	2 kN load					4 kN load				
	Defect size (width) in mm					Defect size (width) in mm				
	0.3	**0.5**	**0.7**	**0.9**	**1.1**	**0.3**	**0.5**	**0.7**	**0.9**	**1.1**
500	0.65	0.58	0.80	0.81	0.74	0.64	0.65	0.70	0.87	0.95
700	0.86	0.83	1.23	1.24	1.10	0.91	0.95	1.04	1.23	1.31
900	1.08	1.20	1.64	1.60	1.47	1.18	1.28	1.49	1.70	1.73
1100	1.38	1.53	2.01	2.27	1.78	1.38	1.72	1.78	2.13	2.25
1300	1.57	1.66	2.27	2.45	2.17	1.84	2.11	2.40	2.66	2.91
1500	2.01	2.01	2.90	2.97	2.57	2.09	2.43	2.70	3.02	3.28

The variations of AE amplitudes and vibration RMS velocities with respect to gradual increase of defect size of all test runs are compared and presented in Tables 4 and 5 and the trends are shown in graphs Figs. 6-7. In VA the overall RMS velocity gradually increases with increase in defect size, load and speed, but the variations are not significant. The same trends are also observed in AE analysis, but the incremental

increase is very significant at defect size and load. In all AE envelope spectrums (Figs. 8 to 12) clear peak rise observed at BPFO and maximum amplitude is recorded but in vibration spectrums (Figs. 13 to 16) no such clear peak is observed. In vibration frequency spectra other peaks observed but they do not belong to bearing defect frequencies.

Table 5. Acoustic Emission amplitude (dB level) at various defect sizes, RPM and Load.

RPM	2 kN load					4 kN load				
	Defect size (width) in mm					Defect size (width) in mm				
	0.3	**0.5**	**0.7**	**0.9**	**1.1**	**0.3**	**0.5**	**0.7**	**0.9**	**1.1**
500	1.14	1.80	2.53	3.01	3.16	1.13	2.04	2.96	3.04	3.98
700	1.30	1.46	2.71	4.22	4.27	1.25	3.43	3.52	4.55	5.96
900	1.08	2.16	3.75	4.99	5.81	1.39	4.32	5.78	6.94	7.41
1100	1.74	2.89	4.58	5.27	6.49	2.18	5.84	5.83	6.95	8.55
1300	2.06	3.21	5.47	5.76	5.98	2.21	4.21	5.31	5.99	9.76
1500	1.84	3.52	4.61	6.76	6.87	2.34	5.07	6.02	6.95	11.8

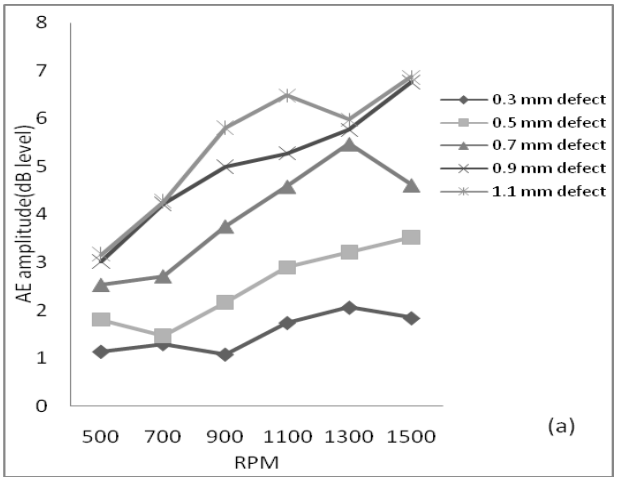

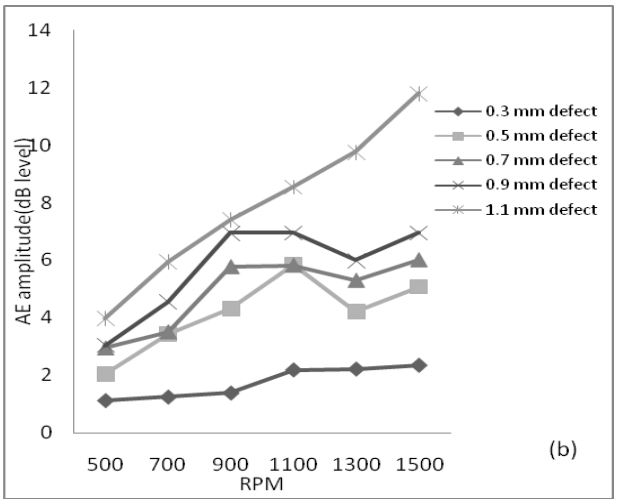

Fig. 6. AE amplitudes at (a) 4 kN load & (b) 2 kN load of different defect sizes and RPM.

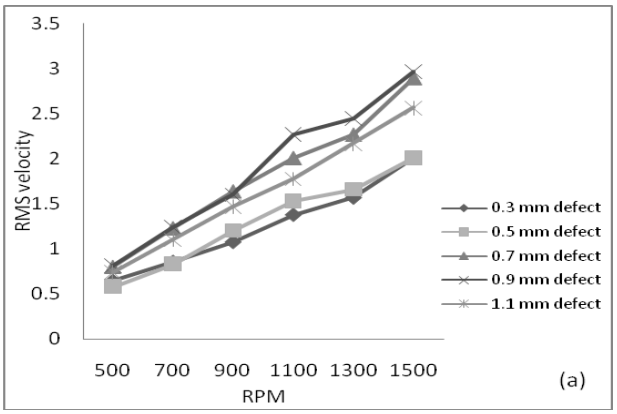

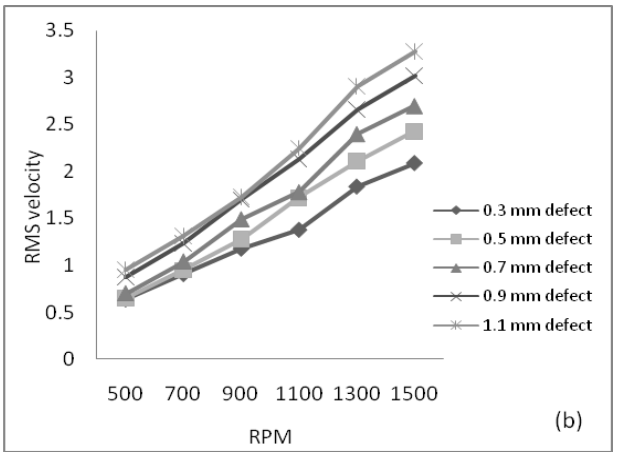

Fig. 7. Vibration RMS velocity (a) 4 kN load & (b) 2 kN load of different defect sizes and RPM.

From the overall experimental data it is found that as defect size increases there is a significant increase in corresponding AE amplitude level. The reason for this phenomenon is, when the defect width size is very small the rolling element can easily roll over the defect, hence there is no much obstruction to the rolling motion and therefore the force exerted by the rolling element over the defect edge is very small. Hence there is little disturbance in the defect area of outer race and the stress caused is very less and negligible. As the defect size increases, the rolling element comes down gradually to the defect that the fault edge obstructs the rolling motion of rolling element and its velocity decreases momentarily. There is a greater change in momentum and so there is more impact over the defect due to rolling element. Due to increase in force, the stress over the defect area increases which may lead to extension of the defect. The stress may even reach the breaking point of the material which can lead to increase in the defect size. Due to this change in energy released at the point of defect in the form of high frequency stress waves these

were captured by the AE probe, but vibration accelerometer is unable to capture these due to its low frequency range. In all AE frequency spectra it is observed that the peaks raised at BPFO and maximum amplitude recorded, but this is not the case in vibration spectrums.

6. CONCLUSION

In this paper the results of present investigation are presented, which is an attempt made to find out the practical AE and vibration response with gradual increase of defect size in bearing outer race. Time waves and frequency spectrums of both methods (bearing without defect and with defects) are analyzed. There is significant difference in vibration and acoustic emission spectrums. In vibration analysis, overall RMS velocity increases with the increase in RPM and load. The same trend is observed with increase in the defect size. From vibration time waves it can be concluded that there is a defect in outer race but the severity of the defect could not be ascertained.

In AE analysis the frequency spectrum clearly shows the defect frequency and subsequent super harmonics. The dB value also increases along with RPM, load and defect size. From the AE time wave the energy released at each impact can be clearly observed. The area under the curve shows the impact which increases with increase in defect size. Hence from these experimental investigations it is revealed that AE technique is superior to vibration technique and gives better analysis to diagnose the defects in bearings. Also AE technique is found useful to characterize and to find out the size of the defect. In continuation of this investigation a mathematical model is being developed to study the influence of all the seeded defects on the behavior of the said bearing theoretically to correlate the experimentally obtained results.

REFERENCES

[1] E.P. Carden and P. Fanning, 'Vibration based condition monitoring: a review', *Structural Health Monitoring*, vol. 3, no. 4, pp. 355–377, 2004.

[2] Ch. Ratnam, J. Srinivas and B.S.N. Murthy, 'Damage detection in mechanical systems using Fourier coefficients', *Journal of sound and vibration*, vol. 303, pp. 909-917, 2007.

[3] Ch. Ratnam and B.S. Ben, 'Structural damage detection using combined finite element and model lamb wave propagation parameters', *Journal of mechanical science*, vol. 223, pp. 769-777, 2009.

[4] P.S. Rao and Ch. Ratnam, 'Vibration based damage identification using Burg's algorithm and Stewart control charts', *Journal of ASTM International*, vol. 8, no. 4, 2011.

[5] S.W. Doebling, C.R. Farrar and M.B. Prime, 'A summary review of vibration based damage identification methods', *Shock and Vibration Digest*, vol. 30, no. 3, pp. 91–105, 1998.

[6] N. Tandon and A. Choudhury, 'A review of Vibration and Acoustic measurement methods for the detection of defects in rolling element bearings', *Tribol. Int.*, vol. 32, no.8, pp. 469-80, 1999.

[7] Todorovic Petar, Jeremic Branislav, Macuzic Ivan, Brkovic Aleksandar and Proso Uross, 'Vibration analysis of cracked rotor during run-up', *Tribology in Industry*, vol. 30, no. 1&2, pp. 55-62, 2008.

[8] P.D. McFadden and J.D. Smith, 'Vibration monitoring of rolling element bearings by the high-frequency resonance technique- a review', *Tribology International*, vol. 17, no. 1, pp. 3-10, 1984.

[9] LabVIEW, Advance Digital Signal Processing User Manual, Austin, 2007.

[10] J.R. Mathew, *Acoustic Emission*. Gordon and Breach Science Publishers Inc., New York, 1983.

[11] N.K. Myshkin and D.V. Tkachuk, 'Tribology Development in Russia and Belarus', *Tribology in Industry*, vol. 31, no. 1-2, pp. 3-7, 2009.

[12] A. Minewitsch, 'Some Developments in Triboanalysis of Coated Machine Components', *Tribology in Industry*, vol. 33, no. 4, pp. 153-158, 2011.

[13] T. Yoshioka and T. Fujiwara, 'New acoustic emission source locating system for the study of rolling contact fatigue', *Wear*, vol. 81, no. 1, pp. 183–186, 1982.

[14] T. Yoshioka and T. Fujiwara, 'Application of acoustic emission technique to detection of rolling bearing failure', *American Society of Mechanical Engineers*, vol. 14, pp. 55–76, 1984.

[15] D. Mba, R.H. Bannister and G.E. Findlay, 'Condition monitoring of low-speed rotating machinery using stress waves, Parts I and II',

Proceedings of the Institution of Mechanical Engineers, vol. 213, no. 3, pp. 153–185, 1999.

[16] N. Jamaludin, D. Mba and R.H. Bannister, 'Condition monitoring of slow-speed rolling element bearings using stress waves'*, Journal of Process Mechanical Engineering, Proceedings of the Institution of Mechanical Engineers, Part E: Journal of Process Mechanical Engineering*, vol. 215, no. 4, pp. 245–271, 2001.

[17] T.J. Holroyd and N. Randall, 'Use of acoustic emission for machine condition monitoring', *British Journal of Non- Destructive Testing*, vol. 35, no. 2, pp. 75–78, 1993.

[18] T. Holroyd, 'Condition monitoring of very slowly rotating machinery using AE techniques', in: *14th International Congress on Condition Monitoring and Diagnostic Engineering Management*, Manchester, paper 29, UK, 4–6 September 2001.

[19] S. Bagnoli and C.R Citti, 'Comparison of accelerometer and acoustic emission signals as diagnostic tools in assessing bearing', in: *Proceedings of Second International Conference on Condition Monitoring*, London, UK, May 1988, pp. 117–125.

[20] S. Orhan, N. Akturk and V. Celik, 'Vibration monitoring for defect diagnosis of rolling element bearings as a predictive maintenance tool: Comprehensive case studies', *NDT&E International*, vol. 39, no. 4, pp. 293–298, 2006.

[21] Jong-Eok Ban, Byoung-Hoo Rho and Woong Kim, 'A study on the sound of roller bearings operating under radial load', *Tribology International*, vol. 40, no. 1, pp. 21–28, 2007.

[22] M. Bains and M. Kumar, 'Detection of missing ball in bearing using decomposition of acoustic signal', *Asian Journal of Chemistry*, vol. 21, no. 10, pp. 143-147, 2009.

[23] S.R. Messer, J. Agzarian and D. Abbott, 'Optimal wavelet denoising for phonocardiograms', *Microelectronics Journal*, vol. 32, no. 12, pp. 931–941, 2001.

[24] A.M. Al-Ghamd and D. Mba, 'A comparative experimental study on the use of acoustic emission and vibration analysis for bearing defect identification and estimation of defect size', *Mechanical Systems and Signal Processing*, vol. 20, no. 7, pp. 1537–1571, 2006.

[25] H. Prasad, 'The effect of cage and roller slip on the measured defect frequency response of rolling element bearings', *ASLE Trans*, vol. 30, no. 3, pp. 360-367, 1987.

[26] A.B. Johnson and A.F. Stronach, 'Bearing fault detection in hostile environment', in: *I Proceedings of International Conference on Condition Monitoring*, Brighton, UK, 21-23 May, pp. 35-44, 1986.

[27] T. Williams, X. Ribadeneira, S. Billington and T. Kurfess, 'Rolling Element Bearing Diagnostics in Run-To Failure Lifetime Testing', *Mechanical Systems and Signal Processing*, vol. 15, no. 5, pp. 979–993, 2001.